

Prevalence of American Heart Association Type VI Carotid Atherosclerotic Lesions Identified by Magnetic Resonance Imaging for Different Levels of Stenosis as Measured by Duplex Ultrasound

Tobias Saam, MD,*† Hunter R. Underhill, MD,† Baocheng Chu, MD, PhD,†
Norihide Takaya, MD, PhD,† Jianming Cai, MD, PhD,† Nayak L. Polissar, PhD,‡
Chun Yuan, PhD,† Thomas S. Hatsukami, MD§
Munich, Germany; and Seattle, Washington

- Objectives** Via magnetic resonance imaging (MRI), we sought to determine the prevalence of atherosclerotic American Heart Association type VI lesions (AHA-LT6) (lesions with luminal surface defect, hemorrhage/thrombus, or calcified nodule) in carotid arteries that represented all categories of stenosis as measured by duplex ultrasound.
- Background** Arterial stenosis alone has been shown to be a poor predictor of cardiovascular events. Autopsy studies suggest that features associated with AHA-LT6 lesions, rather than the degree of luminal narrowing, characterize the high-risk plaque.
- Methods** A total of 192 subjects underwent bilateral carotid artery magnetic resonance imaging (MRI) scans at 1.5T after evaluation with ultrasound to determine stenosis. After excluding arteries with a previous endarterectomy, poor image quality, or missing ultrasound data, there were 175 patients with 260 arteries available for analysis. The AHA lesion type was determined by the consensus opinion of 2 experienced carotid MRI reviewers.
- Results** In total, 96 of 260 (37.0%) arteries had ≥ 1 location with AHA-LT6. Of the arteries with AHA-LT6, 84.4% had hemorrhage, 45.8% had a ruptured fibrous cap, and 14.6% showed other type of complications. Prevalence of AHA-LT6 was an increasing sequence of 8.1% in the 37 arteries with 1% to 15% stenosis, 21.7% in the 60 arteries with 16% to 49% stenosis, 36.8% in the 114 arteries with 50% to 79% stenosis, and 77.6% in the 49 arteries with 80% to 99% stenosis.
- Conclusions** Complicated AHA-LT6 are frequently found in arteries with $\leq 50\%$ stenosis. These findings indicate that complex lesions develop in a substantial number of arteries in the absence of high-grade stenosis. Ongoing prospective studies will determine the predictive value of vulnerable plaque features, as visualized by MRI, for risk of subsequent ischemic events. (J Am Coll Cardiol 2008;51:1014–21) © 2008 by the American College of Cardiology Foundation

Stroke is the third most common cause of mortality in the U.S., with an incidence of approximately 700,000 deaths per year. As a means to prevent cerebrovascular events, current medical doctrine advocates endarterectomy in patients with advanced carotid disease (1). Although the established criteria for surgical intervention are presently driven by the

severity of carotid luminal stenosis and a patient's symptom status, there is increasing evidence showing that luminal narrowing may be a poor predictor of lesion vulnerability. The Asymptomatic Carotid Atherosclerosis Study (2), which randomized 1,662 patients with carotid artery stenosis of 60% or greater to surgery or medical therapy, found that only 1 stroke per year was prevented for every 85 patients undergoing endarterectomy. Moreover, results from the NASCET (North American Symptomatic Carotid Endarterectomy Trial) showed that of the 2,226 symptomatic eligible patients with $<70\%$ stenosis, 61% had $<50\%$ stenosis and 19% had $<30\%$ stenosis (3).

Therefore, alternative criteria have been sought to better identify patients most at risk of complications from carotid disease. From surgical and post-mortem tissue, the concept

From the *Department of Clinical Radiology, University of Munich, Grosshadern Campus, Munich, Germany; †Department of Radiology, University of Washington, Seattle, Washington; ‡The Mountain-Whisper-Light Statistical Consulting, Seattle, Washington; and the §VA Puget Sound Health Care System and Department of Surgery, University of Washington, Seattle, Washington. Supported by National Institutes of Health grants R01 HL61851, R01 HL073401, P01 HL072262, R01HL56874, and T32 HL07828.

Manuscript received July 5, 2007; revised manuscript received August 30, 2007, accepted October 15, 2007.

of the vulnerable plaque has emerged and the characterization of high-risk lesions as plaques with the presence of a surface disruption, hemorrhage, or calcified nodule has been increasingly accepted (4–7). Although the prevalence of these complex features has been studied in carotid endarterectomy specimens (8), little is known about their prevalence in subjects with <50% stenosis because of an inability in the past to visualize the morphology and composition of the in vivo arterial wall.

Magnetic resonance imaging (MRI) has shown great promise in characterizing carotid atherosclerotic lesions (9–11). In particular, MRI has been proven to comprehensively evaluate the in vivo complications of the atherosclerotic plaque, such as fibrous cap rupture (12), hemorrhage/thrombus (13–15), and calcified nodules (10). Furthermore, MRI has also been shown to reproducibly (16) characterize the American Heart Association lesion type (AHA-LT) according to modified MRI criteria (17).

In this investigation, we used high-resolution MRI to evaluate the carotid arterial wall from subjects that represented the full spectrum of arterial stenosis by duplex ultrasound. Specifically, we sought to determine the prevalence of complicated AHA-LT6 (plaques with luminal surface defect, hemorrhage/thrombus, or calcified nodules) for each category of stenosis in the carotid artery.

Methods

Subjects. Between 1998 and 2005, 192 subjects had their bilateral carotid arteries imaged with high-resolution MRI. Subjects were recruited from the diagnostic vascular ultrasound laboratories at the University of Washington Medical Center and the Veterans Affairs Puget Sound Health Care System after obtaining their informed consent (mean age 68 years; 24 females) (Table 1). The study procedures and consent forms were reviewed and approved by each site’s

institutional review board before study initiation. Arteries were excluded from review if there was: 1) missing duplex ultrasound data of the artery; 2) a prior carotid endarterectomy or carotid stenting; 3) history of cervical radiation therapy; 4) insufficient coverage of the bifurcation by MRI; 5) <1% stenosis or >99% stenosis as measured by duplex ultrasound; or 6) poor image quality (ImQ) by MRI.

Duplex ultrasound. Subjects underwent duplex ultrasound examination at the diagnostic vascular ultrasound laboratories at the University of Washington Medical Center and the Veterans Affairs Puget Sound Health Care System. Duplex categories were determined according to Strandness criteria (18) (Table 2), and arteries were grouped into the following degrees of stenosis: 1% to 15% stenosis (n = 37), 16% to 49% stenosis (n = 60), 50% to 79% stenosis (n = 114), and 80% to 99% stenosis (n = 49).

MRI protocol. Patients were imaged using a 1.5T MRI scanner (Signa Horizon EchoSpeed, General Electric Healthcare, Waukesha, Wisconsin) and bilateral phased-array surface coils (Pathway MRI, Seattle, Washington) (19). Fast-spin echocardiography-based T1-, proton density (PD)-, and T2-weighted images as well as 3-dimensional (3D) time-of-flight (TOF) images of the bilateral carotid arteries were obtained using a previously published standardized protocol (11).

All images were obtained with a field of view of 13 cm to 16 cm, matrix size of 256 × 256, slice thickness of 2 mm, interslice spacing of 0 mm (–1 mm for 3D TOF; only every second image of TOF images was used for analysis), and 2 signal averages (best in plane pixel size 0.50 × 0.50 mm² to 0.62 × 0.62 mm², depending on field of view). The scan was centered on the bifurcation of the artery with greater stenosis. Fat suppression was used for T1-, PD-, and T2-weighted images to reduce signal from subcutaneous fat.

MRI image review and criteria. Five reviewers (N.T., J.C., B.C., H.U., T.S.), all with more than 1.5 years experience in carotid plaque imaging, performed the image review. Each scan was interpreted by 2 reviewers reaching a consensus opinion. Reviewers were blinded to subject information, duplex ultrasound results, and clinical information. An ImQ rating (5-point scale: 1 = poor, 5 = excellent) was assigned to all magnetic resonance images before the review (10). Imaging locations with an average ImQ < 3, principally caused by subject motion or low signal-to-noise ratio, were excluded from the study. Lumen and wall area measurements were performed by all 5 reviewers, whereas the evaluation of AHA-LT6 and the type of complication was evaluated by 2 reviewers (T.S., H.U.).

Abbreviations and Acronyms

- 3D** = 3-dimensional
- AHA** = American Heart Association
- ImQ** = image quality
- LT** = lesion type
- MRI** = magnetic resonance imaging
- NWI** = normalized wall index
- PD** = proton-density
- TOF** = time-of-flight

Table 1 Clinical Data and Risk Factors (175 Patients)

Demographics and Risk Factors	n	Mean ± SD or %	Range (If Applicable)
Age, yrs	175	68.0 ± 9.0	41–87
Male, %	175	86.3%	
Height, m	159	1.74 ± 0.08	1.50–1.96
Weight, kg	164	81.5 ± 15.1	49–131
Body mass index, kg/m ²	159	26.9 ± 4.2	17.5–40.7
Hypertension, %	171	81.3%	
Diabetes, %	173	24.9%	
Smoking status	170		
Active, %		32.4%	
Quit, %		37.1%	
Never smoked, %		30.6%	
History of coronary artery disease, %	165	37.6%	
Hypercholesterolemia, %	170	84.1%	
Family history of coronary artery disease, %	131	45.0%	
Statins, %	173	73.4%	

n = number of patients with available information; SD = standard deviation.

Category	Diameter Reduction (%)	Velocity Criteria	Flow Characteristics
A	0	PSV <125 cm/s	Minimal or no spectral broadening; flow separation within bulb often detected; no plaque visualized on B-mode
B	1-15	PSV <125 cm/s	Minimal spectral broadening; plaque visualized on B-mode image
C	16-49	PSV <125 cm/s	Spectral broadening fills the systolic window; plaque visualized on B-mode
D	50-79	PSV ≥125 cm/s	Marked spectral broadening often detected
D+	80-99	EDV ≥140 cm/s	Marked spectral broadening
E	Occlusion	NA	No flow detected in ICA; occlusive signal with low or reversed diastolic flow in CCA

Doppler signals acquired 60° angle to vessel axis with 5-MHz probe and small sample volume. Diameter reduction used the diameter of the carotid bulb as denominator. Data from Roederer et al. (18).

CCA = common carotid artery; EDV = end diastolic velocity; ICA = internal carotid artery; PSV = peak systolic velocity.

For area measurements, the lumen and outer vessel wall boundaries (total vessel area) were manually traced using a custom-designed image analysis tool QVAS (20). The total vessel area included the lumen and wall areas. The wall area for each location was calculated as the difference between the total vessel and lumen areas. The normalized wall index (NWI) was calculated as wall area divided by the outer wall area. The complicated AHA-LT6 was determined according to previously published criteria (17), based on relative tissue intensities in TOF, T1-, T2-, and PD-weighted images, and the appearance of the luminal surface. An AHA-LT6 is a complex plaque with luminal surface defect (fibrous cap rupture with or without ulceration), intraplaque hemorrhage, juxtaluminal hemorrhage/mural thrombus, or calcified nodules projecting into the lumen, as described by Virmani et al (5).

Criteria for determining the occurrence of hemorrhage was based on previously published carotid MRI criteria (13-14). Briefly, type I hemorrhage is hyperintense on TOF and T1-weighted images and isointense to hypointense on PD- and T2-weighted images. Type II hemorrhage has high signal intensity on all 4 weightings. Hemorrhage/thrombus was considered to be juxtaluminal (14) if the region of interest was adjacent to the lumen, and the dark juxtaluminal band was absent on the TOF images.

The fibrous cap was categorized as ruptured (12) if the lumen boundary on TOF and T1-, PD-, and T2-weighted images was irregular and the dark band on TOF images was disrupted or if the dark band on TOF images was not visible and a hyperintense, bright signal adjacent to the lumen on TOF images indicating the presence of juxtaluminal thrombus/hemorrhage was present. Ulceration was identified by an irregular luminal surface on all contrast weightings. A location was considered to have a penetrating ulcer if 2 flow channels separated by a membrane were seen on TOF images.

Calcification was identified as a hypointense signal on all 4 weightings. Calcified nodules were not discernable from the lumen on the black blood images, but were

clearly distinguishable from the bright lumen in the TOF images (10).

To assess intrareader and interreader reproducibility, 32 arteries of 32 distinct subjects were re-evaluated 4 weeks after the initial review by the same pair of reviewers who did the first review and by a second pair of reviewers.

Data analysis. For each imaged location, the AHA-LT6 and the type of complication, such as fibrous cap rupture, juxtaluminal hemorrhage/thrombus, calcified nodules, or penetrating ulcer leading to the type VI classification, was documented. For each artery, AHA-LT6 was considered to be present if at least 1 imaged location showed features of a complicated plaque. An artery with more than 1 complicated location did not receive additional weighting. For each duplex category, the prevalence of AHA-LT6 was calculated.

The prevalence of AHA-LT6 was also analyzed for each segment of the artery. Arterial segments were defined as: 1) common: >4 mm proximal to the bifurcation; 2) carotid bulb: 0 mm to 4 mm proximal to the bifurcation; and 3) internal: ≥2 mm distal to the bifurcation. To compare the prevalence of AHA-LT6 between the common and internal carotid artery and the carotid bulb, we used logistic regression. The AHA-LT6 was the dependent variable, coded as present versus absent for each location. The 3 artery segments (common, bulb, internal) were represented as a categorical independent variable. Statistical significance was determined from the contrast between pairs of the 3 segment categories. The logistic regression analysis was carried out using generalized estimating equations to accommodate the multiple locations per artery and the 2 arteries for some patients. A Spearman correlation coefficient (rho) with the artery as the unit of analysis was used to correlate quantitative plaque measurements with the occurrence of complicated plaque features. A conservative value of statistical significance for the Spearman rho was calculated using the 2-tailed *t* distribution, Fisher *z*-transform of rho [$Z_{rho} = 0.5 \times \log_e ((1 + rho)/(1 - rho))$], the estimated standard error (SE) for the transformed value of

ρ [$SE = 1/\sqrt{(n - 3)}$], and $t = Z_{\rho}/SE$ with $n - 3$ degrees of freedom. The sample size (n) for this calculation was conservatively set at the number of patients rather than the considerably larger sample size of arteries.

To quantify the intrareader and interreader reproducibility for the AHA lesion type, Cohen kappa (κ) was computed. For this reproducibility assessment, each artery was rated as having versus not having a location with a type VI lesion. All analyses were performed with SPSS for Windows (version 12.0; SPSS, Inc., Chicago, Illinois), STATA (version 8.2; StataCorp, LP College Station, Texas), and the statistical language R (version 2.5.0; R Foundation for Statistical Computing, Vienna, Austria).

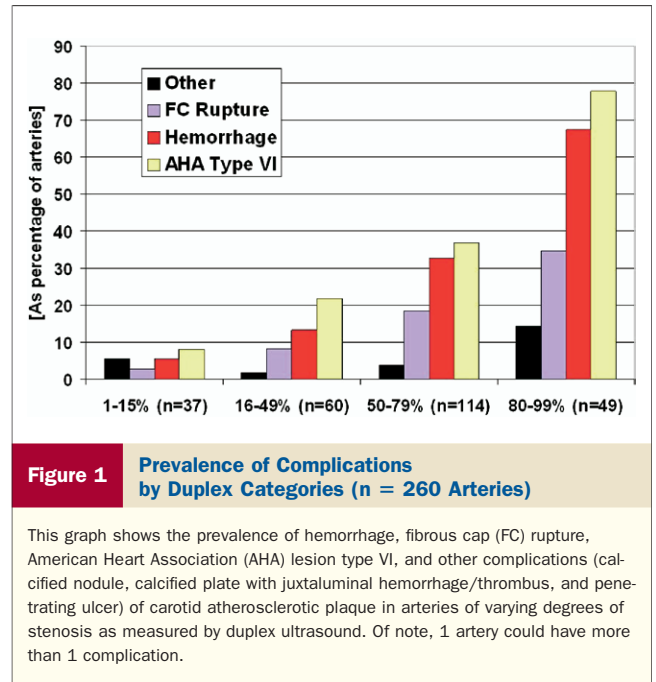
Results

Artery selection. Ten percent of all subjects scanned at our institution during the indicated period of investigation had nondiagnostic scans with an $ImQ \leq 3$ and were a priori excluded from analysis. There were 175 subjects with 350 arteries available for evaluation. Of the 350 arteries, 90 carotid arteries were excluded for the following reasons: 1) prior carotid endarterectomy ($n = 18$), 2) missing ultrasound data ($n = 26$), 3) carotid bifurcation covered only on one side ($n = 19$), 4) $<1\%$ stenosis ($n = 6$) by duplex ultrasound, 5) $>99\%$ stenosis ($n = 3$) by duplex ultrasound, and 6) nondiagnostic images on one side ($n = 18$). Consequently, there were 260 evaluable arteries with a total of 2,504 imaging locations, which resulted in a mean coverage of 1.93 cm per artery.

Prevalence of AHA-LT6 according to duplex categories. In total, 96 of 260 (37.0%) arteries had ≥ 1 location with AHA-LT6. Of the 96 arteries with AHA-LT6, 84.4% (81 arteries) had hemorrhage, 45.8% (44 arteries) had a ruptured fibrous cap, and 13.5% (13 arteries) showed other types of complications. A ruptured fibrous cap never occurred without MRI presence of intraplaque hemorrhage. Of the 13 arteries that showed other types of complications, 9 had calcified nodules, 3 had an intraluminal thrombus, and 1 had a penetrating ulcer. In 2 cases the calcified nodule was associated with a fibrous cap rupture.

Figure 1 shows the prevalence of hemorrhage, fibrous cap rupture, AHA-LT6, and others (calcified nodule, penetrating ulcer) by duplex category. Carotid prevalence of AHA-LT6 was 8.1% in the 37 arteries with 1% to 15% stenosis, 21.7% in the 60 arteries with 16% to 49% stenosis, 36.8% in the 114 arteries with 50% to 79% stenosis, and 77.6% in the 49 arteries with 80% to 99% stenosis. Examples of AHA-LT6 are shown for arteries with 1% to 15% and 16% to 49% stenosis in Figures 2 and 3.

Location of AHA-LT6 lesions. Complicated lesions were most commonly found at the bifurcation or 1 location below or above the bifurcation, with a prevalence of nearly 25% at these locations (Fig. 4). Overall, AHA-LT6 had a significantly higher prevalence in locations of carotid bulb compared with the common (21.0% vs. 6.8%, $p < 0.001$) and



internal carotid artery (21.0% vs. 16.8%, $p = 0.006$). An AHA-LT6 was more common in locations of internal than common carotid artery ($p < 0.001$).

Prevalence of plaque components. Prevalence of lipid-rich/necrotic core increased substantially with higher degrees of stenosis. In fact, 91.8% of all subjects with 80% to 99% stenosis had a lesion with a lipid-rich/necrotic core (Table 3). Even in subjects with $<50\%$ stenosis, lipid-rich/necrotic cores were frequently found. Prevalence of calcification was lowest in subjects with 1% to 15% stenosis at 43.2%, but did not vary substantially in subjects with higher degrees of stenosis.

Prevalence of AHA-LT6 and the relationship to arterial remodeling. There were highly significant negative correlations between minimum lumen area and AHA-LT6, intraplaque hemorrhage, and fibrous cap rupture. Furthermore, there were highly significant positive correlations between maximum wall area/maximum NWI and AHA-LT6, intraplaque hemorrhage, and fibrous cap rupture (Table 4). Spearman correlation coefficients for the relationship between quantitative plaque measurements and the occurrence of complications were highest for maximum NWI, followed by minimum lumen area, and lowest for maximum wall area. Intraplaque hemorrhage showed a stronger correlation with these quantitative measurements than fibrous cap rupture. No significant correlations between occurrence of complicated plaque features and maximum total vessel area were observed. Prevalence of AHA-LT6 in arteries with $<50\%$ stenosis was substantially higher at the site of maximum wall area compared with the site of minimum lumen area (9.3% vs. 1%).

Figure 4 shows the percentage occurrence at each location of the artery's maximum wall area, minimum lumen area,

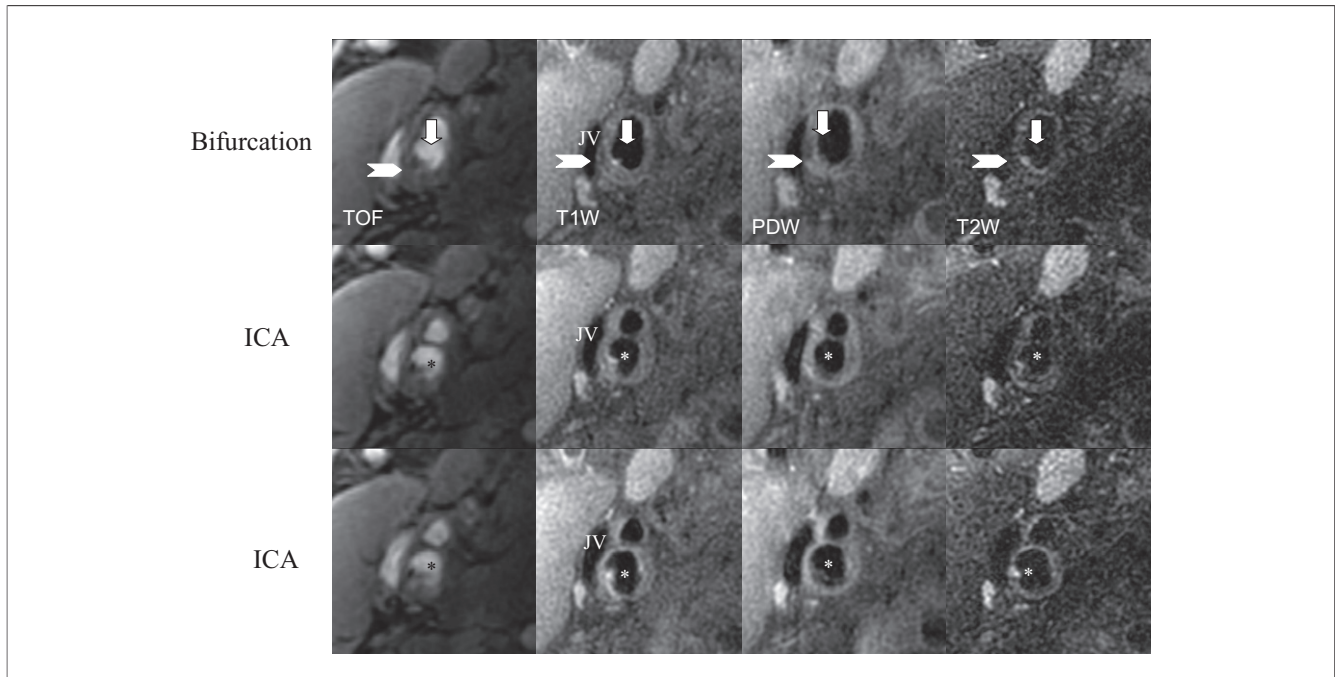


Figure 2 Complicated Atherosclerotic Plaque in the Right Carotid Artery in a Subject With 1% to 15% Stenosis

The **chevron** points to an eccentric plaque with a lipid/necrotic core without hemorrhage. The **arrow** points to a hyperintense area in T1- and T2-weighted images, indicating the presence of juxtaluminal hemorrhage/thrombus. The irregular surface of the plaque can best be depicted on the TOF images (the **asterisks** indicate the lumen). ICA = internal carotid artery; JV = jugular vein; PDW = proton-density weighted; TOF = time-of-flight.

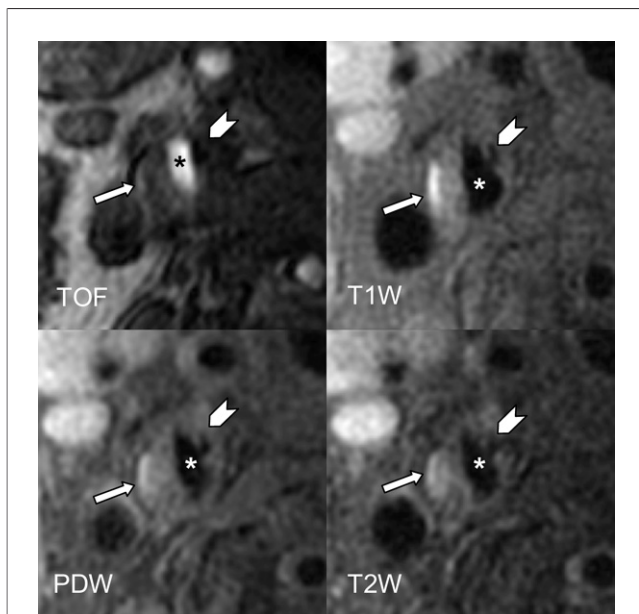


Figure 3 Complicated Internal Carotid Plaque in a Subject With 16% to 49% Stenosis

The **asterisks** indicate the lumen of the internal carotid artery; the **chevron** points to an area that is hypointense on all 4 weightings, indicating the presence of juxtaluminal calcification; and the **arrow** points to an area of high signal intensity on all 4 weightings, indicating the presence of type II hemorrhage. Abbreviations as in Figure 2.

and maximum NWI. The locations of greatest luminal narrowing do not correspond well to and occur more distal to the locations with a higher prevalence of type VI lesions and maximum wall area and NWI.

Reproducibility of AHA lesion type. The reproducibility analysis was based on 32 arteries in 32 subjects; 5 of the arteries were noted by at least 1 of the reviewers as having a type VI lesion. The intrareader and interreader reproducibility for the modified AHA lesion type VI was very good, with κ values of 1.0 and 0.87, respectively.

Discussion

This cross-sectional study used multisequence high-resolution MRI to reproducibly evaluate the prevalence of complicated AHA-LT6 in 260 arteries with varying degrees of stenosis as measured by duplex ultrasound. Although the prevalence of AHA-LT6 was more prominent in the most stenotic vessels, there was a relatively high occurrence of complex features in lesions with only $\leq 50\%$ stenosis. Furthermore, over 20% of arteries with high-grade, 80% to 99% stenosis did not have type VI lesions. These findings show that not all plaques of similar stenosis are the same, and highlight the need for direct evaluation of the vessel wall for improved discrimination of culprit lesions in patients with all classifications of carotid stenosis.

Of the features that define the AHA-LT6, hemorrhage and fibrous cap rupture were the most prominent complications identified. Although prospective studies are needed

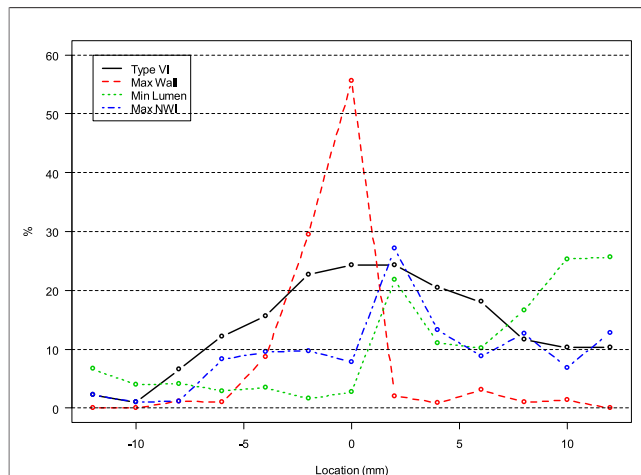


Figure 4 Prevalence of Complicated AHA Type VI Lesions at Each MR Imaging Location

This graph shows the prevalence of complicated AHA type VI lesions at each MR imaging location with the x axis indicating the distance from the bifurcation and the locations of the minimum lumen area, maximum wall area, and maximum NWI for the artery. Locations from -12 to -6 mm were located in the common carotid artery, locations from -4 to 0 mm were located in the carotid bulb, and locations from 2 to 12 mm were located in the internal carotid artery; 2,378 locations are represented. AHA = American Heart Association; MR = magnetic resonance; NWI = normalized wall index.

to identify the importance of these components in lesions with 50% stenosis, their prominent frequency in all categories clearly indicates the possibility of plaque instability independent of stenotic severity. In subjects with 50% to 79% stenosis, the impact of complicated plaque features on plaque progression and future cerebrovascular events has been evaluated in 2 prospective studies (21,22). A recent longitudinal MRI study of 31 patients (21) showed that hemorrhage into the carotid plaque accelerated plaque progression in a period of 18 months. The percent change in wall volume (6.8% vs. -0.15%, $p = 0.009$) and lipid/necrotic core volume (28.4% vs. -5.2%, $p = 0.001$) was significantly higher in the hemorrhage group as compared with the control group (21). Further, patients with intraplaque hemorrhage at baseline showed a far greater susceptibility to repeat plaque hemorrhages (21). Moreover, in a recent prospective MRI study (22) of 154 subjects with asymptomatic 50% to 79% carotid stenosis by duplex ultrasound, the association of complicated plaque features with the development of cerebrovascular events was investigated. Intraplaque hemorrhage, large necrotic cores, and/or a thin or ruptured fibrous cap were strongly associated with future cerebrovascular events. As such, early identification of individuals with these types of complications may enable more aggressive therapy to retard progression or identify individuals at greater risk who need more frequent evaluation.

It is important to observe that the prevalence of these features may be even higher than reported herein. In a meta-analysis of studies based on carotid endarterectomy

specimens in subjects with >50% stenosis (8), prevalence of hemorrhage ranged from 17% to 93% with a mean prevalence of 49%, and prevalence of ulceration/fibrous cap rupture ranged from 17% to 74%, with a mean prevalence of 40%. In a comparable subset of our patient population with 50% to 99% stenosis, the mean prevalence of hemorrhage was 42%, and the mean prevalence of fibrous cap rupture was 18.4% and 34.7% for subjects with 50% to 79% and 80% to 99% stenosis, respectively. Our reported prevalence of complicated plaque features is slightly lower compared with histopathology studies, which is not surprising because histology enables the identification of small surface disruptions and hemorrhages beyond the resolution of MRI.

We found the prevalence of AHA-LT6 to be greatest in the carotid bulb; however, Figure 4 clearly shows that complex lesions may develop in any segment of the carotid artery. Complex lesions were identified at a higher incidence in the arterial wall both 1 cm proximal and distal to the bifurcation. This finding indicates the importance of capturing all segments of the artery during imaging investigations to adequately assess lesion stability.

Significant correlations were found for the prevalence of complications and quantitative plaque measurements, such as minimum lumen area, maximum wall area, and maximum NWI. Previous studies have shown that NWI might be a useful imaging parameter for assessing atherosclerotic disease severity because it takes into account lumen area stenosis and an increased wall area (23). Consistent with this notion, we found the highest correlation coefficients between quantitative plaque measurements and complicated plaque features for maximum NWI. Interestingly, no significant correlation between maximum total vessel area and occurrence of complicated plaque features was found, suggesting that outward remodeling might have a relatively small impact on the occurrence of complicated plaque features in carotid arteries.

Beyond the key findings associated with AHA-LT6, plaque compositional analysis yielded several interesting results. We found that although the prevalence of the lipid-rich/necrotic core was greatest in the most stenotic vessels, its occurrence remained notably high even in subjects with <50% stenosis. This finding shows that substantial changes in the composition of the atherosclerotic wall occur before significant luminal narrowing.

Dissimilar to the other components, calcification did not conform to a specific trend. The prevalence of calcification was >40% in all the evaluated duplex categories. Addition-

Table 3 Prevalence of Plaque Components Based on 260 Arteries Grouped by Duplex Categories

Plaque Component (%)	1-15 (n = 37)	16-49 (n = 60)	50-79 (n = 114)	80-99 (n = 49)
Lipid-rich/necrotic core	43.2	58.3	76.3	91.8
Calcification	43.2	78.3	71.1	73.5

Values represent the percentage per artery, averaged across all arteries.
 n = number of arteries.

Table 4 Correlation of Quantitative Plaque Area Measurements With the Occurrence of Complicated Plaque Features Based on 260 Arteries

Spearman Correlation Coefficient	AHA-LT6	Hemorrhage	Fibrous Cap Rupture	Other Types of Complications*
Minimum lumen area	−0.46 p < 0.001	−0.48 p < 0.001	−0.28 p < 0.001	0 p = 1.0
Maximum wall area	0.29 p < 0.001	0.25 p < 0.001	0.23 p = 0.002	0.1 p = 0.2
Maximum NWI	0.57 p < 0.001	0.56 p < 0.001	0.34 p < 0.001	0.09 p = 0.2
Maximum total vessel area	−0.07 p = 0.4	0.1 p = 0.2	0 p = 1.0	0 p = 1.0

*Calcified nodules/plates, thrombus, and penetrating ulcer.
AHA-LT6 = American Heart Association lesion type VI; NWI = normalized wall index.

ally, 26.5% of all subjects with 80% to 99% stenosis did not show any calcification by MRI. As such, the impact of calcification on a plaque’s vulnerability in the carotid atherosclerotic lesion remains unclear and requires prospective evaluation to determine whether calcification is a plaque stabilizing or destabilizing feature.

Study limitations. The subjects in this study were recruited from the diagnostic vascular ultrasound laboratory and had carotid disease identified by duplex ultrasound. Therefore, the prevalence of complicated AHA-LT6 is likely to be lower in the general population without known carotid artery disease.

Also, only MRI examinations of at least average image quality (image quality ≥ 3) were considered for review, resulting in the exclusion of approximately 10% of all subjects from analysis. Recent improvements in pulse sequence design and in coil design have already decreased the number of exclusions in subjects scanned more recently, and high-field MRI shows great promise to further decrease the number of exclusions.

Our multisequence imaging protocol was optimized for visualization of plaque characteristics and had a coverage ranging from 2.4 cm for the T1-weighted images and 5.2 cm for the TOF images. Therefore, it was not possible to measure luminal stenosis using conventional criteria, as described in the NASCET trial, because of the absence of a nondiseased reference segment distal to the stenosis within the field of view. However, duplex ultrasound is able to reliably measure luminal stenosis with good correlation to digital subtraction angiography (24). Improvement in temporal resolution and signal to noise ratio by 3D MRI will allow larger coverage of the carotid artery and will permit assessment of luminal stenosis using NASCET criteria.

Conclusions

Complicated AHA-LT6 with hemorrhage, fibrous cap rupture, or calcified nodules are frequently found in arteries with $\leq 50\%$ stenosis. These findings indicate that complex lesions develop in a substantial number of arteries in the

absence of high-grade stenosis. Prospective studies in subjects with $\leq 50\%$ stenosis will determine the predictive value of vulnerable plaque features, as visualized by MRI, for risk of subsequent ischemic events.

Reprint requests and correspondence: Dr. Thomas S. Hatsukami, VA Puget Sound Health Care System, Surgery and Perioperative Care (112), 1660 South Columbian Way, Seattle, Washington 98108. E-mail: tomhat@u.washington.edu.

REFERENCES

- Moore WS, Barnett HJ, Beebe HG, et al. Guidelines for carotid endarterectomy. A multidisciplinary consensus statement from the ad hoc committee, American Heart Association. *Circulation* 1995;91:566–79.
- Endarterectomy for asymptomatic carotid artery stenosis. Executive Committee for the Asymptomatic Carotid Atherosclerosis Study. *JAMA* 1995;273:1421–1428.
- Barnett HJ, Taylor DW, Eliasziw M, et al. Benefit of carotid endarterectomy in patients with symptomatic moderate or severe stenosis. North American Symptomatic Carotid Endarterectomy Trial Collaborators. *N Engl J Med* 1998;339:1415–25.
- Stary HC, Chandler AB, Dinsmore RE, et al. A definition of advanced types of atherosclerotic lesions and a histological classification of atherosclerosis. A report from the Committee on Vascular Lesions of the Council on Arteriosclerosis, American Heart Association. *Circulation* 1995;92:1355–74.
- Virmani R, Kolodgie FD, Burke AP, Farb A, Schwartz SM. Lessons from sudden coronary death: a comprehensive morphological classification scheme for atherosclerotic lesions. *Arterioscler Thromb Vasc Biol* 2000;20:1262–75.
- Naghavi M, Libby P, Falk E, et al. From vulnerable plaque to vulnerable patient: a call for new definitions and risk assessment strategies: part I. *Circulation* 2003;108:1664–72.
- Naghavi M, Libby P, Falk E, et al. From vulnerable plaque to vulnerable patient: a call for new definitions and risk assessment strategies: part II. *Circulation* 2003;108:1772–8.
- Golledge J, Greenhalgh RM, Davies AH. The symptomatic carotid plaque. *Stroke* 2000;31:774–81.
- Saam T, Ferguson MS, Yarnykh VL, et al. Quantitative evaluation of carotid plaque composition by in vivo MRI. *Arterioscler Thromb Vasc Biol* 2005;25:234–9.
- Yuan C, Mitsumori LM, Ferguson MS, et al. In vivo accuracy of multispectral magnetic resonance imaging for identifying lipid-rich necrotic cores and intraplaque hemorrhage in advanced human carotid plaques. *Circulation* 2001;104:2051–6.
- Yuan C, Mitsumori LM, Beach KW, Maravilla KR. Carotid atherosclerotic plaque: noninvasive MR characterization and identification of vulnerable lesions. *Radiology* 2001;221:285–99.

12. Hatsukami TS, Ross R, Polissar NL, Yuan C. Visualization of fibrous cap thickness and rupture in human atherosclerotic carotid plaque in vivo with high-resolution magnetic resonance imaging. *Circulation* 2000;102:959–64.
13. Chu B, Kampschulte A, Ferguson MS, et al. Hemorrhage in the atherosclerotic carotid plaque: a high-resolution MRI study. *Stroke* 2004;35:1079–84.
14. Kampschulte A, Ferguson MS, Kerwin WS, et al. Differentiation of intraplaque versus juxtaluminal hemorrhage/thrombus in advanced human carotid atherosclerotic lesions by in vivo magnetic resonance imaging. *Circulation* 2004;110:3239–44.
15. Moody AR, Murphy RE, Morgan PS, et al. Characterization of complicated carotid plaque with magnetic resonance direct thrombus imaging in patients with cerebral ischemia. *Circulation* 2003;107:3047–52.
16. Chu BC, Hatsukami TS, Zhao XQ, et al. Reproducibility of carotid atherosclerotic lesion type determination using high-resolution magnetic resonance imaging (abstr). *Atheroscler Suppl* 2003;4:253.
17. Cai JM, Hatsukami TS, Ferguson MS, Small R, Polissar NL, Yuan C. Classification of human carotid atherosclerotic lesions with in vivo multicontrast magnetic resonance imaging. *Circulation* 2002;106:1368–73.
18. Roederer GO, Langlois YE, Jager KA, et al. A simple spectral parameter for accurate classification of severe carotid disease. *Bruit* 1984;8:174–8.
19. Hayes CE, Mathis CM, Yuan C. Surface coil phased arrays for high-resolution imaging of the carotid arteries. *J Magn Reson Imaging* 1996;6:109–12.
20. Kerwin W, Xu D, Liu F, et al. Magnetic resonance imaging of carotid atherosclerosis: plaque analysis. *Top Magn Reson Imaging*. 2007;18:371–8.
21. Takaya N, Yuan C, Chu B, et al. Presence of intraplaque hemorrhage stimulates progression of carotid atherosclerotic plaques: a high-resolution magnetic resonance imaging study. *Circulation* 2005;111:2768–75.
22. Takaya N, Yuan C, Chu B, et al. Association between carotid plaque characteristics and subsequent ischemic cerebrovascular events: a prospective assessment with MRI—initial results. *Stroke* 2006;37:818–23.
23. Saam T, Yuan C, Chu B, et al. Predictors of carotid atherosclerotic plaque progression as measured by noninvasive magnetic resonance imaging. *Atherosclerosis* 2007;194:e34–42.
24. Nederkoorn PJ, van der GY, Hunink MG. Duplex ultrasound and magnetic resonance angiography compared with digital subtraction angiography in carotid artery stenosis: a systematic review. *Stroke* 2003;34:1324–32.